

Multiwavelength Raman spectroscopy of diamond nanowires present in *n*-type ultrananocrystalline films

R. Arenal,^{1,2,*} G. Montagnac,³ P. Bruno,² and D. M. Gruen²

¹Laboratoire d'Etude des Microstructures, ONERA-CNRS, 92322 Châtillon, France

²Materials Science Division, Argonne National Laboratory, Illinois 60439, USA

³Laboratoire de Sciences de la Terre, Ecole Normale Supérieure de Lyon, Lyon 69364, France

(Received 7 August 2007; revised manuscript received 12 October 2007; published 17 December 2007)

Multiwavelength Raman spectroscopy is employed to investigate ultrananocrystalline diamond films deposited by the plasma enhanced chemical vapor deposition technique. Recently, we have shown that the addition of nitrogen in the gas source during synthesis induce the formation of diamond *n*-type films, exhibiting the highest electrical conductivity at ambient temperature. This point is related with the formation of elongated diamond nanostructures and the presence of sp^2 -bonded carbon in these films. The Raman results presented here confirm these aspects and provide a better and deeper understanding of the nature of these films and their related optical and electronic properties.

DOI: 10.1103/PhysRevB.76.245316

PACS number(s): 78.30.-j, 81.05.Uw, 72.20.-i, 81.07.-b

I. INTRODUCTION

Nanodiamond materials have been the subject of high scientific interest in recent years due to their unique physical properties.^{1,2} In this sense, ultrananocrystalline diamond (UNCD) films are very promising nanostructured carbon materials. Such films consist of nanosized grains composed of 3–5 nm randomly oriented diamond crystallites surrounded by 0.2–0.3 nm wide grain boundaries.¹ These films are suitable as hard coatings on machine tools and rotating shaft seals. Recently, UNCD microelectromechanical system resonators have been shown to operate at frequencies considerably higher than similar resonators made of silicon and have very high Q values.³

UNCD films are synthesized from argon microwave plasmas containing 1% carbon in the form of C_{60} or CH_4 and are highly electrically insulating.¹ The progressive substitution of nitrogen for argon in the synthesis gas renders the films increasingly electrically conducting with conductivities reaching several hundred S/cm for 20% by volume of N_2 added to the synthesis gas.^{4–8} In our recent work, we showed that such electronic modifications, which are strongly correlated with the increase of nitrogen gas contents, are promoted by morphological changes. For more than 10% by volume of N_2 added to the synthesis gas, one observes the formation of diamond fibers.⁸ As their presence is related to the increasing electrical conductivity of the films, reaching several hundred S/cm, they are called nanowires. It was also shown that the remarkable increase in conductivity is associated with the fact that each nanowire is enveloped by an amorphous sheath. The sheath is composed of largely sp^2 -bonded carbon as assessed by electron energy loss spectroscopy (EELS) measurements. We suggest that the sheath and other sp^2 -bonded carbon material existing in those UNCD films are responsible for the high conductivity.

Raman spectroscopy is a nondestructive technique which provides useful information in materials in general^{9–11} and in carbon materials, in particular, such as sp^2/sp^3 ratio, density, sp^2 sites ordering,^{10,12–17} etc. Indeed, the optical, electrical, and mechanical properties of any carbon material depend on

the medium-range ordering, which comprises the degree of sp^2 clusters, the bond angle and length distortion, and the ordering inside the clusters.^{12–17}

Visible Raman scattering from carbons is mainly sensible to the sp^2 sites and less to the sp^3 bonding ones. That is due to the proximity of the visible laser wavelength to the band gap of sp^2 carbon atoms that leads to resonance enhancement in the corresponding Raman cross section.¹² In fact, sp^2 sites have a cross section for visible Raman more than 50 times larger than sp^3 sites.¹³ To overcome this problem, UV Raman spectroscopy was performed, in addition to visible Raman, to increase the sensitivity to sp^3 -bonded carbon through resonance enhancement of these atomic sites.

In this paper, we present a detailed multiwavelength Raman spectroscopy study on these UNCD *n*-type films. We improve the knowledge of these materials in the case where nitrogen is substituted for argon in the synthesis gas. This study is necessary in order to understand their transition from insulators to metal-like behavior (exhibiting a high conductivity).

II. EXPERIMENT

UNCD films were synthesized using microwave plasma enhanced chemical vapor deposition (MWPECVD) process. These films were grown on both Si and Si/SiO₂ wafers. The substrate temperature was 800 °C. Ar/CH₄/N₂ plasmas were investigated here with a nominal gas composition of 1% for CH₄ and variable Ar and N₂ flow rates so that the total gas flow was always 100 SCCM (SCCM denotes cubic centimeter per minute at STP). The nitrogen content was varied in the range between 0% and 20%. The electrical conductivity values of these films vary between 10⁻⁷ and 200 Ω cm⁻¹ for 0% and 20% of N₂ added, respectively.⁸

Unpolarized Raman spectra were excited with 514.5 and 632.8 nm of an argon-ion and He-Ne lasers, respectively, and were recorded by the Jobin-Yvon Labram HR800 visible spectrometer in backscattering geometry at room temperature. This Raman system consists of a microscope with 100× objective lens, which allows a spot size of ~1 μm.

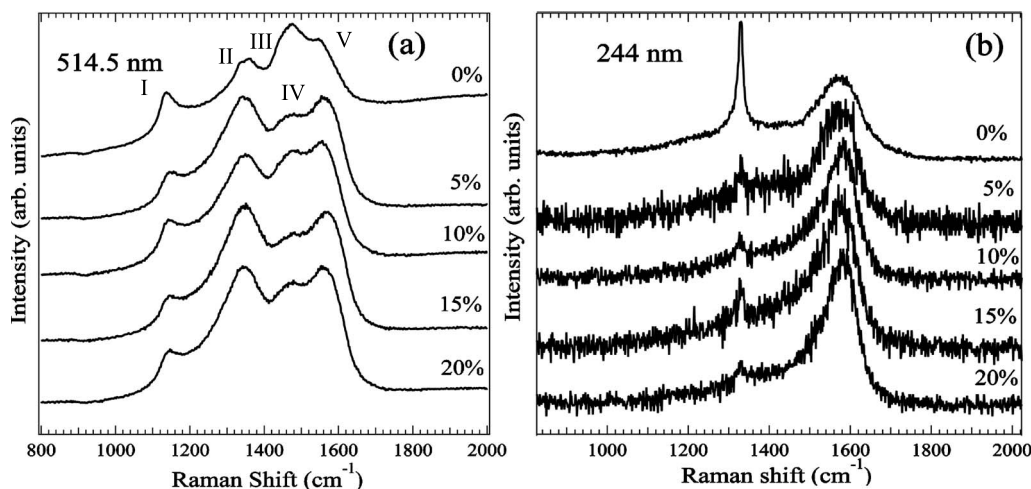


FIG. 1. Raman spectra at two different wavelengths of different UNCD films where nitrogen addition in the synthesis gas increases from 0% to 20% (substrate temperature of 800 °C during deposition): (a) 514.5 nm and (b) 244 nm.

Unpolarized UV spectra were collected at room temperature and excited by the 244 nm line of a frequency doubled argon-ion laser using Jobin-Yvon Labram HR800 UV spectrometer. A 40 \times objective lens was employed providing a spatial resolution of $\sim 2 \mu\text{m}$. In all the cases, we used low laser power density at the surface of the sample and short acquisition time in order to avoid damage. These parameters were kept the same for all samples. Spectral resolutions were 1 and 6 cm^{-1} for visible and UV excitations, respectively.

III. RESULTS

Figure 1(a) shows the Raman spectra recorded at 514.5 nm on different UNCD films where the percentage of N_2 gas during synthesis varies from 0% to 20%. Typical UNCD Raman features can be seen for all these samples. They consist of four distinctive peaks at 1140 (marked as I in this figure), 1345 (marked as III), ~ 1480 (marked as IV), and $1550\text{--}1580 \text{ cm}^{-1}$ (marked as V). The pair of peaks at $1550\text{--}1580$ and 1345 cm^{-1} are assigned to the G and D peaks of sp^2 -bonded carbon, respectively. The former corresponds to a bond-stretching vibration of a pair of sp^2 sites (in the form of olefinic chains or of aromatic rings), whereas the latter (D peak) is an A_{1g} breathing mode of a sixfold aromatic ring, which is activated by disorder.¹² For the peaks centered at 1140 and $\sim 1480 \text{ cm}^{-1}$, they correspond, respectively, to the C-H bending and to the C-C stretching Raman modes of *trans*-polyacetylene (*t*-PA or poly- CH_x).^{18–22} The *t*-PA is an alternate chain of sp^2 carbon atoms, with a single hydrogen bonded to each carbon atom and this *t*-PA is lying in the grain boundary of UNCD crystallites.^{19,21,22} In addition to these features, there is a peak at 1332 cm^{-1} [marked as II in Fig. 1(a)]. This peak corresponds to the sp^3 sites (T_{2g} mode). The low cross section of the sp^3 -bonded carbon in the visible wavelength justifies the weak signal of this peak. Furthermore, we observe that this peak is clearly visible for the samples with 0% and 5% of N_2 , but it is not the case for the rest of the samples. This result indicates the increase of the quantity of the sp^2 -bonded carbon with the amount of nitro-

gen added to the synthesis gas. Similar result has been observed by Vlasov *et al.*²² In the same way, we observe an increase of the Raman scattering with the increase of nitrogen in the synthesis gas. This result confirms the increase of the sp^2 fraction for these samples as Achatz *et al.* pointed out by optical absorption measurements.²³ All these features in the Raman scattering at the visible excitation indicate that the overall structure of UNCD films is dominated by the sp^2 sites in the presence of sp^3 -bonded carbon as well as *t*-PA chains.

Turning to the analysis of the UV Raman results [see Fig. 1(b)], a very interesting point is the strong signal of the diamond peak at 1332 cm^{-1} in the spectra at 0% and the absence of this signal for the rest of the samples. As we know from our previous transmission electron microscopy (TEM) studies [selected area electron diffraction (SAED), high-resolution TEM (HRTEM), and EELS],⁸ the addition of nitrogen induces the formation in these films of diamond nanowires which are surrounded by a sp^2 carbon sheath and embedded in a matrix composed by UNCD grains. Thus, the absence of this peak at 1332 cm^{-1} for the UV excitation wavelength, particularly where one would expect the resonance enhancement of sp^3 -bonded carbon for these *n*-type UNCD films, indicates that the presence of highly optically absorbing sp^2 -bonded carbon strongly decreases the scattered Raman radiation intensity. Alternatively, the low Raman intensity due to sp^3 centers can be explained by the shallow penetration depth of UV light in these materials (only a few nanometers).²⁴ We note that this is not the case in the visible excitation wavelength because the penetration depth of visible light is $1\text{--}2 \mu\text{m}$.

Figure 2(a) displays the Raman spectra obtained at 632.8 nm of the two extreme samples, with 0% and 20% of N_2 , respectively. These results are an extra proof of the existence of *t*-PA in these films. In this plot, we superpose to these spectra those recorded at 514.5 nm to show the dispersion (modification of the position of the peaks as a function of the excitation energy) of the two modes at 1140 and 1480 cm^{-1} of these polymeric chains. The behavior of these

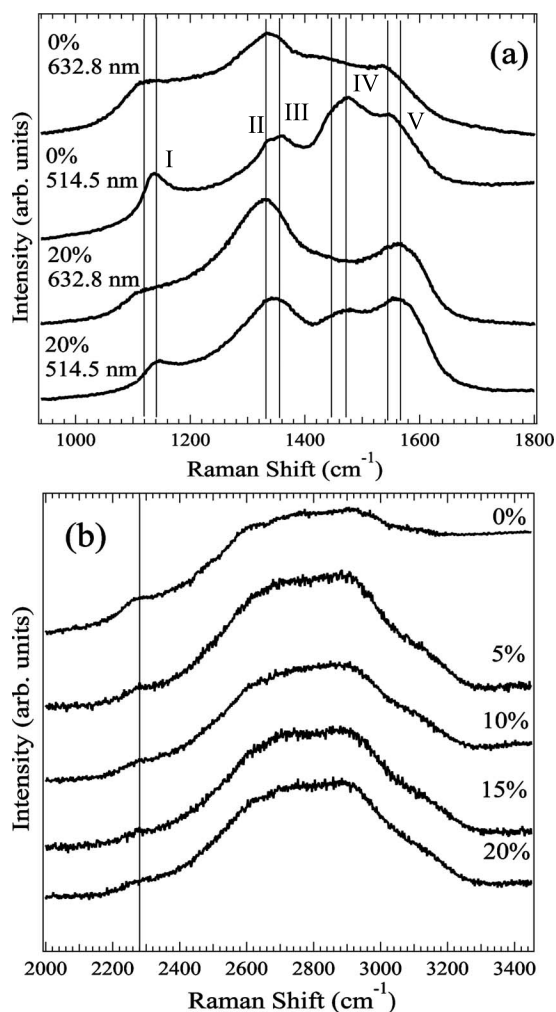


FIG. 2. (a) 514.5 and 632.8 nm Raman spectra of two different UNCD samples: 0% and 20% nitrogen additions. (b) Second order Raman spectra recorded at 514.5 nm of different UNCD samples where nitrogen addition in the synthesis gas increases from 0% to 20% (substrate temperature of 800 °C during deposition).

peaks with respect to the wavelength [Fig. 2(a)] was pointed out recently by several authors.²¹ On the other hand, it is interesting also to point out the dispersion shown by the *D* peak in these spectra. The dispersion of this peak is proportional to the order of *sp*² sites¹³: the dispersion increases for increasing order.

In the region of higher-order Raman spectra, a broad band in the range of 2500–3200 cm⁻¹ is observed for all these UNCD films [Fig. 2(b)]. Three lines can be distinguished in this spectral region which correspond to the second order Raman of disordered *sp*²-bonded carbon, presenting a mixture of overtones of the 1350 and 1550 cm⁻¹ modes and their combination.¹³ In these spectra, another weak band at 2275 cm⁻¹ is visible. This corresponds to the second order Raman of *trans*-polyacetylene.²² In addition to this line, other combination and overtones of other modes from *t*-PA could be present in the broad band between 2500 and 3200 cm⁻¹ described previously but they are masked or overlapped with the other modes from the overtones of the *sp*²-bonded carbons. It is interesting also to note that the

intensity of this peak at 2275 cm⁻¹ is decreasing with the increasing of the N₂ addition to the synthesis gas.

The atomic concentration of nitrogen in the films is less than 1% even if the N₂ addition in the gas is 20%.^{25,26} It is known that the effects of low amounts of nitrogen on the Raman scattering, as we are dealing with here, are to induce π bonds and *sp*² clustering on carbon material.¹³ In addition, even if different kinds of nitrogen bonding in carbon nitrides (pyrrole, pyridine, or graphitelike) could be considered, the vibration frequencies of these solid systems are expected to be close to those of the pure carbon ones, 1300–1600 cm⁻¹ for aromatic *sp*² rings and 1500–1600 cm⁻¹ for olefinic chains. Thus, in this region of 1300–1600 cm⁻¹, there is no particular signal that we could distinguish from these modes compared with those coming from the carbon structures, and we neglect the contribution of those C-N and N-N modes.

In order to know about the carbon bonding, clustering, and order of the *sp*² sites as a function of nitrogen addition, we monitored several parameters: the position, the width [full width at half maximum (FWHM)], and the dispersion [variation of the position of the peak as a function of the excitation energy, *Disp*(*G*)] of the *G* peak, as well as the intensity ratio of the *D* and *G* peaks, *I*(*D*)/*I*(*G*). Using Gaussian fits, we have studied all these parameters considering N-free systems for the reasons invoked above. We justify the choice for our fitting procedure using Gaussian line shape because this shape is expected for a random distribution of phonon lifetimes in disorder materials as we are dealing with here.^{12,27,28}

Figure 3(a) shows the position of the *G* peak with N₂ addition for 514.5 and 244 nm excitation wavelengths. This parameter is related with the bonding strength.^{13,29} It can be seen that this the peak is upshifted with the increase of N₂ addition for both excitation wavelengths, visible and UV. We attribute this upshift to the increase of clustering in these films with nitrogen addition.

The ratio between the intensity of the *D* and *G* peaks [*I*(*D*)/*I*(*G*)] provides a measure of the ordering of the *sp*²-bonded carbon. In our case [Fig. 3(b)], as the nitrogen addition increases, the long range ordering in the *sp*² sites increases and the *D* peak becomes more prominent. Moreover, the *D* peak intensity is quite sensitive to the cluster size and, as the cluster size increases, this intensity decreases with respect to that of the *G* peak. Thus, from *I*(*D*)/*I*(*G*), it is possible, using an empirical expression,¹² to estimate the size of the clusters (or the in-plane correlation length *L*_a). In our case, they vary from 11 to 14.5 Å with N₂ addition [see Fig. 3(b)]. These *L*_a values correspond to approximately five aromatic rings per cluster. Thus, the analysis of this parameter provides information about the number of aromatic rings in the cluster which, as we show, increases with nitrogen addition.

The width of the *G* peak (FWHM in our case) reflects the bond length and angle distortion.^{12,13,17,27} In Fig. 4(a), for both excitation wavelengths, FWHM decreases gradually with nitrogen addition. This indicates that the graphitic clusters become larger and more ordered, in agreement with the size dependence (higher *L*_a). On the other hand, as expected, the FWHM of the *G* peak is lower for UV excitation. Lower excitation wavelengths are resonant with smaller clusters and then FWHM(*G*) decreases with lambda.^{13,27}

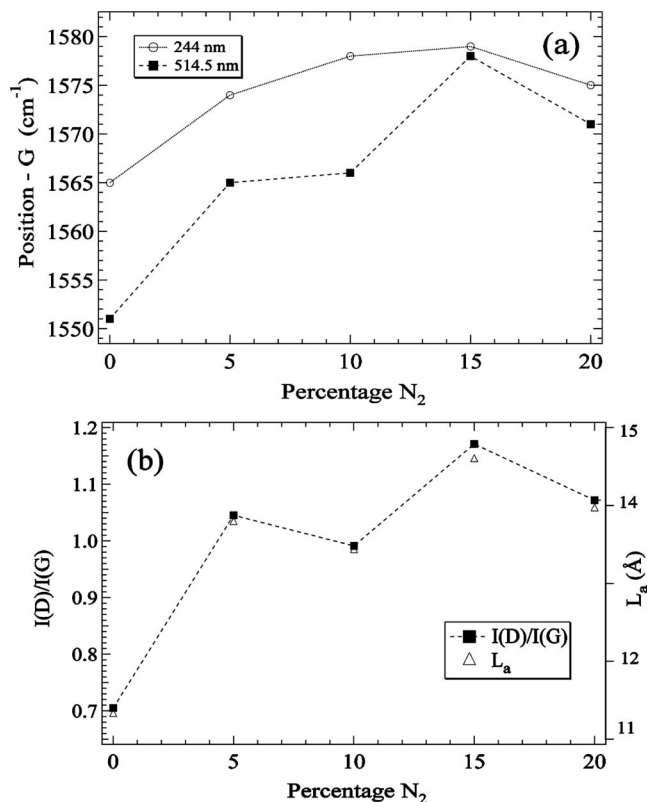


FIG. 3. (a) Variation of the G peak position with nitrogen addition in the synthesis gas of UNCD films. (b) Variation of the D to G peaks intensity ratio $[I(D)/I(G)]$ for these UNCD films.

Figure 4(b) shows the dispersion of the G peak position, $\text{Disp}(G)$. This parameter gives an idea of the topological order (size and shape) of the sp^2 clusters.²⁷ This value is zero when no sp^2 bonds exist in the form of chains and only perfect rings are present. That is due to the fact that the bond lengths of the olefinic sp^2 chains are shorter than those of the aromatic sp^2 groups. Thus, they have higher vibrational frequencies and their contribution to the UV Raman scattering (short wavelengths) must be larger due to the resonance phenomenon.^{27,30} In such case, their response is hardly affected by the wavelength employed. From our results, we conclude that the G peak comes only from the response of the aromatic rings and that these chains are not present in our films. Moreover, this also means that the films are composed of sp^2 rings with the π bonds fully delocalized, and this delocalization increases as a function of the added N_2 .^{12,27} The electronic delocalization is strongly supported by the measurements of Mares *et al.* on giant negative magnetoresistance.³¹

Figure 5(a) shows the position of the G peak against the $I(D)/I(G)$ ratio. There is a linear relationship between those parameters. This plot confirms that the clustering increases with N_2 addition. Furthermore, a similar trend is shown in Fig. 5(b) where we plot the FWHM of the G peak as a function of the $I(D)/I(G)$ ratio. From this figure, we conclude that the order of the graphitelike clusters increases as well as the size of those rings.

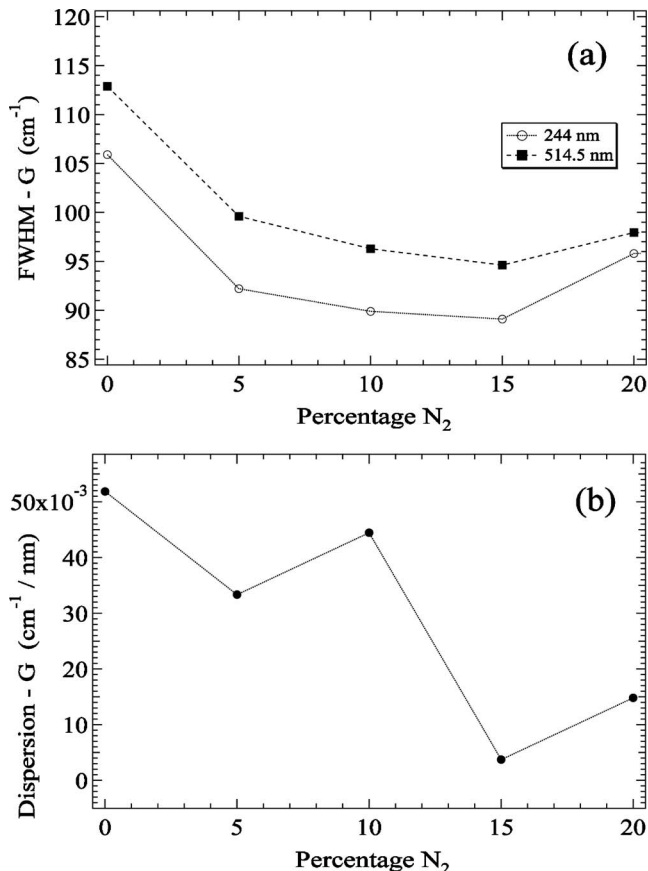


FIG. 4. (a) FWHM of the G peak for UNCD films as a function of nitrogen addition in the synthesis gas. (b) Dispersion of the G peak for these UNCD films.

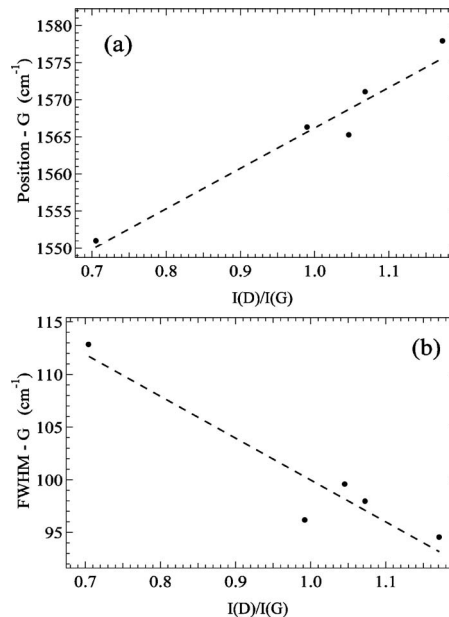


FIG. 5. (a) Variation of the G peak position against $I(D)/I(G)$ for these UNCD films. (b) Plot of the $\text{FWHM}(G)$ versus $I(D)/I(G)$.

IV. DISCUSSION

The progressive substitution of nitrogen for argon in the synthesis gas in these UNCD films provokes morphological changes and electronic modifications of the UNCD films.^{5,8,25} As we invoked before, the electrical conductivity of the films increases with the increase of nitrogen. In fact, these films constitute the highest currently available *n*-type diamond material that is electrically conducting at ambient temperatures with conductivity values of several hundred S/cm for 20% by volume of added N₂. The abrupt change in conductivity behavior suggests a microstructural transformation that could account for the occurrence of the insulator-metal transition. Our recent TEM studies (HRTEM, SAED, and EELS) showed the formation of diamond nanowires and the presence of a significant fraction of *sp*² atoms, some of them in the form of a carbon sheath surrounding the nanowires (NWs).

Optical and electrical properties of carbon materials presenting a mixture *sp*²-/*sp*³-bonded carbon as is the case of UNCD, diamondlike carbon, or CN_x films are correlated with the degree of clustering (size, density, and order).^{12,13,17} Furthermore, from recent works, it is known that nitrogen incorporation into a carbon network has significant effects on the aromatic clustering kinetics: changing the bonding length compared with the pure carbon network and enhancing the order in a disordered carbon network.^{13,29} Our present studies confirm those aspects. The lack of dispersion of the position of the *G* peak indicates that the clusters are only composed of *sp*² aromatic rings. The upshifting of the *G* peak and the narrowing of its peak width with nitrogen addition in the synthesis gas indicate the increase of the *sp*² fraction in the films. Moreover, the trends of the FWHM of the *G* peak are similar for 244 and 514.5 nm excitation wavelengths, decreasing as a function of the addition of N₂ in the gas phase. This indicates an increase of the structural order, inducing a decrease in the bond length and angle distortion.^{13,14,29} On other hand, the ratio between the intensities of the *D* and *G* peaks, $I(D)/I(G)$, provides information about the delocalization of the π bonds in these rings. This value is different from zero indicating that the π bonds are delocalized and this delocalization increases as a function of the added nitrogen.²⁷ It is known that the gap is controlled by the π -electron delocalization.^{12,31} Thus, this result confirms previous results showing the electronic weak localization for these films.³¹

The absence of any feature corresponding to the *sp*³-bonded carbon in the UV Raman spectra for the samples

where nitrogen is added indicates the presence of material which prevents the scattering of the diamond sites. This confirms our TEM (EELS and HRTEM) results showing the presence of a *sp*² sheath surrounding the diamond NWs.⁸ We suggest that the presence of this *sp*² layer justifies the lack of signal of the *sp*³ atoms in the UV Raman spectra. Moreover, as we pointed out in our recent work,⁸ this *sp*²-bonded carbon sheath provides a plausible transport mechanism for electronic conductivity to occur. This point, in addition to the results presented here and concerning the *sp*² clustering, is crucial to understand the high conductivity values shown by of these *n*-type UNCD films.

V. CONCLUSION

Visible and UV Raman spectroscopies were used to investigate UNCD films deposited by MWPECVD on Si and Si/SiO₂ substrates at 800 °C with 0%, 5%, 10%, 15%, and 20% nitrogen substitutions for Ar in the synthesis gas. Therefore, this multiwavelength Raman study that we carried out allows a direct correlation of the Raman parameters with N₂ addition at the gas source, which is not possible for single wavelength excitation. The Raman characteristics and structural changes in the films were studied as a function of this progressive substitution of nitrogen for argon.

From these studies, we conclude that the addition of nitrogen to the synthesis gas, besides the formation of the diamond NWs that we reported recently,⁸ promotes the *sp*² aromatic clustering, the increase of the size of these clusters, and the enhancement of their ordering. Furthermore, the UV Raman studies confirm the presence of *sp*²-bonded carbon in the films, preventing the Raman scattering of the *sp*³ sites. This is a supplementary proof to the existence of carbon sheath surrounded the diamond NWs which represents an excellent path for the electrons. We confirmed also the presence of *trans*-polyacetylene in these films. All these results explain the electronic modifications observed on these UNCD films when nitrogen reaches 10% in volume or more: optical absorption and electrical conductivity.^{6,8,31,32} Thus, the present study improves our knowledge of the composition and structure of *n*-type UNCD films and provides further insight into the interesting properties of these films.

ACKNOWLEDGMENT

This work was supported by the U.S. Department of Energy, Office of Science, under Contract No. DE-AC02-06CH11357.

*Corresponding author. raul.arenal@onera.fr

¹D. M. Gruen, *Annu. Rev. Mater. Sci.* **29**, 211 (1999).

²O. A. Shenderova and D. M. Gruen, *Ultrananocrystalline Diamond* (William Andrew, New York, 2006).

³S. Srinivasan, J. Hiller, B. Kabius, and O. Auciello, *Appl. Phys. Lett.* **90**, 134101 (2007).

⁴S. Bhattacharyya, O. Auciello, J. Birrell, J. A. Carlisle, L. A.

Curtiss, A. N. Goyette, D. M. Gruen, A. R. Krauss, J. Schlueter, A. Sumant, and P. Zapol, *Appl. Phys. Lett.* **79**, 1441 (2001).

⁵J. Birrell, J. A. Carlisle, O. Auciello, D. M. Gruen, and J. M. Gibson, *Appl. Phys. Lett.* **81**, 2235 (2002).

⁶P. Achatz, O. A. Williams, P. Bruno, D. Gruen, J. A. Garrido, and M. Stutzmann, *Phys. Rev. B* **74**, 155429 (2006).

⁷O. A. Williams, *Semicond. Sci. Technol.* **21**, R49 (2006).

- ⁸R. Arenal, P. Bruno, D. J. Miller, M. Bleuel, J. Lal, and D. M. Gruen, *Phys. Rev. B* **75**, 195431 (2007).
- ⁹M. Cardona and G. Guntherodt, *Light Scattering in Solids* (Springer, New York, 1982).
- ¹⁰S. Reich, C. Thomsen, and J. Maultzsch, *Carbon Nanotubes: Basic Concepts and Physical Properties* (Wiley-VCH, Berlin, 2004).
- ¹¹R. Arenal, A. C. Ferrari, S. Reich, L. Wirtz, J.-Y. Mevellec, S. Lefrant, A. Rubio, and A. Loiseau, *Nano Lett.* **6**, 1812 (2006).
- ¹²A. C. Ferrari and J. Robertson, *Phys. Rev. B* **61**, 14095 (2000).
- ¹³A. C. Ferrari and J. Robertson, *Phys. Rev. B* **64**, 075414 (2001).
- ¹⁴S. E. Rodil, A. C. Ferrari, J. Robertson, and W. I. Milne, *J. Appl. Phys.* **89**, 5425 (2001).
- ¹⁵D. Roy, M. Chhowalla, N. Hellgren, T. W. Clyne, and G. A. J. Amaratunga, *Phys. Rev. B* **70**, 035406 (2004).
- ¹⁶A. C. Y. Liu, R. Arenal, and X. Chen, *Phys. Rev. B* **76**, 121401(R) (2007).
- ¹⁷R. Arenal and A. C. Y. Liu, *Appl. Phys. Lett.* **91**, 211903 (2007).
- ¹⁸T. Lopez-Rios, E. Sandre, S. Leclerq, and E. Sauvain, *Phys. Rev. Lett.* **76**, 4935 (1996).
- ¹⁹A. C. Ferrari and J. Robertson, *Phys. Rev. B* **63**, 121405 (2001).
- ²⁰R. Pfeiffer, H. Kuzmany, N. Salk, and B. Gunther, *Appl. Phys. Lett.* **82**, 4149 (2003).
- ²¹H. Kuzmany, R. Pfeiffer, N. Salk, and B. Gunther, *Carbon* **42**, 911 (2004).
- ²²I. I. Vlasov, V. G. Ralchenko, E. Goovaerts, A. V. Saveliev, and M. V. Kanzyuba, *Phys. Status Solidi A* **203**, 3028 (2006).
- ²³P. Achatz, J. A. Garrido, M. Stutzmann, O. A. Williams, D. M. Gruen, A. Kromka, and D. Steinmuller, *Appl. Phys. Lett.* **88**, 101908 (2006).
- ²⁴S. Gupta, B. R. Weiner, W. H. Nelson, and G. Morell, *J. Raman Spectrosc.* **34**, 192 (2003).
- ²⁵J. Birrell, J. E. Gerbi, O. Auciello, J. M. Gibson, D. M. Gruen, and J. A. Carlisle, *J. Appl. Phys.* **93**, 5606 (2003).
- ²⁶R. Arenal, O. Stephan, P. Bruno, and D. M. Gruen (unpublished).
- ²⁷C. Casiraghi, A. C. Ferrari, and J. Robertson, *Phys. Rev. B* **72**, 085401 (2005).
- ²⁸M. A. Tamor and W. C. Vassell, *J. Appl. Phys.* **76**, 3823 (1994).
- ²⁹G. Abrasonis, R. Gago, M. Vinnichenko, U. Kreissig, A. Kolitsch, and W. Mller, *Phys. Rev. B* **73**, 125427 (2006).
- ³⁰K. W. R. Gilkes, H. S. Sands, D. N. Batchelder, J. Robertson, and W. I. Milne, *Appl. Phys. Lett.* **70**, 1980 (1997).
- ³¹J. J. Mares, P. Hubic, J. Kristofik, D. Kindl, M. Fanta, M. Nesladek, O. Williams, and D. M. Gruen, *Appl. Phys. Lett.* **88**, 092107 (2006).
- ³²S. Bhattacharyya, *Phys. Rev. B* **70**, 125412 (2004).